

Numerical Computation of Resonant Frequency of Shorting Post Loaded Gap-Coupled Circular Microstrip Patch Antennas

Pradeep KUMAR¹, G. SINGH¹, T. CHAKRAVARTY²

¹Department of Electronics and communication Engineering, Jaypee University of Information Technology, Solan, India; ²Embedded Systems Innovation Laboratory, Tata Consultancy Services, Bangalore, India
Email: erpradeep_tiet@yahoo.co.in

Received April 17th, 2009; revised May 30th, 2009; accepted June 5th, 2009.

ABSTRACT

In this paper, the numerical computation of resonant frequency of the two gap-coupled circular microstrip patch antenna loaded with shorting post by using cavity model is presented. The numerically computed results are compared with simulated results. The two gap-coupled circular microstrip patch antenna loaded with shorting post miniaturize the cross-sectional dimension of the radiating patch at the microwave frequency, which is useful for short range communications or contactless identification systems. The simulation has been performed using method-of-moments based commercially available simulator IE3D.

Keywords: Gap-Coupling, Microstrip Antennas, Shorting Post, Resonant Frequency

1. Introduction

An explosive growth of the wireless radio frequency identification market such as electronic toll collection and more generally wireless road-to-vehicle communication systems is currently observed in the microwave band. In the short range communications or contactless identification systems, antennas are key components, which must be small, low profile, and with minimal processing costs [1,2]. The microstrip patch antennas are of great interest for aforementioned mentioned applications due to their thin and compact structures. The flexibility afforded by microstrip antenna technology has led to a wide variety of design and techniques. The main limitations of the microstrip antennas are low efficiency and narrow impedance bandwidth. The bandwidth of the microstrip antenna can be increased using various techniques such as by loading a patch, by using a thicker substrate, by reducing the dielectric constant, by using gap-coupled multi-resonator etc [3–5]. However, using a thicker substrate causes generation of spurious radiation and there are some practical problems in decreasing the dielectric constant. The spurious radiation degrades the antenna parameters. Among various antenna bandwidth enhancement configurations, the two gap-coupled circular microstrip patch antenna is most elegant one. So,

gap-coupling is the suitable method for enhancing the impedance bandwidth of the antennas [6,7]. In the configuration of gap-coupled microstrip antennas method, two patches are placed close to each other. The gap-coupled microstrip antennas generate two resonant frequencies and the bandwidth of the microstrip antennas can be increased [6].

There exist a wide range of basic microstrip antenna shapes such as rectangular, circular and triangular patch shapes which are commonly used patches. For these patches, operating at their fundamental mode resonant frequency, are of the dimension of the patch is about half wavelength in dielectric. At lower frequencies the size of the microstrip antennas becomes large. In modern communication systems the compact microstrip patch antennas are desirable. The size of the microstrip antenna can be reduced by shorting the patch. Changing the basic patch shape can give rise to substantial size reduction. Further decrease in size can be obtained by loading the basic shapes by shorting post or slots [8–10].

In [11,12], circular microstrip patch antenna with dual frequency operation is designed by shorting the patch and the results are compared with the conventional circular microstrip antenna (without a shorting post) which shows that the size of the circular microstrip antenna can be reduced for the same frequency application. It is also

observed that the resonant frequency of the circular microstrip antenna with shorting post can be varied by varying its location. In [13,14], it is shown that the loaded circular microstrip antenna has two modes that is TM_{01} and TM_{11} . Recently, we have also designed two gap-coupled circular microstrip patch antenna without shorting post which generates two modes that is TM_{11} and TM_{21} mode [15].

In the present paper, the two gap-coupled circular microstrip patch antenna is loaded with a shorting post to minimize the size of the antenna structure and it is seen that it generates the three modes that is TM_{01} , TM_{11} and TM_{21} . The resonant frequency of TM_{01} mode of the proposed antenna is lower as compared to TM_{11} and TM_{21} mode of the two gap-coupled circular microstrip antennas as reported in [15]. The numerical computation of the resonant frequency of the shorting post loaded two gap-coupled circular microstrip antenna is performed and the results are compared with the simulated results. The simulation is performed by using the IE3D simulator which is based on the method-of-moment. This paper is structured as follows. In Section 2, the geometrical configuration of the two gap-coupled circular microstrip patch antenna is discussed. In Section 3, the proposed antenna is analyzed theoretically. The Section 4 discusses the analytical and simulated results of the proposed antenna. Finally, Section 5 concludes the work.

2. Antenna Configuration

The geometrical configuration of two gap-coupled circular microstrip patch antennas loaded with shorting post is shown in Figure 1. The patch of radius $a = 15$ mm is the feed patch and other patch of radius $d = 15$ mm is the parasitic patch. The parasitic patch is excited by the gap-coupling whereas the feed patch is excited by the probe feeding technique. The parasitic patch introduces another resonance near the main resonance and proper adjustment of the structure parameters, bandwidth can be enhanced. The feed patch is shorted by shorting post of diameter p . The height and permittivity of the substrate is $h = 1.59$ mm and $\epsilon_r = 2.2$, respectively. The gap distance between the adjacent edges of the feed patch and parasitic patch is s .

3. Theory

Now we divide the structure in two concentric regions; region I and region II as shown in Figure.2. The inner radii of region I is $\frac{p}{2}$ and outer radii of region I is ‘a’. The inner radius of region II is ‘b’ and outer radius of region II is ‘c’.

Now, we consider the field expressions for given TM_{np} mode in these two regions [16].

In region I ($\frac{p}{2} \leq r \leq a$):

The solution of the wave equation in cylindrical coordinates for region I gives the field expressions as:

$$E_z^{(1)} = -j\omega\mu[C_1J_n(kr) + C_2N_n(kr)]\cos n\phi \quad (1)$$

$$H_\phi^{(1)} = -k[C_1J'_n(kr) + C_2N'_n(kr)]\cos n\phi \quad (2)$$

The expression for $H_r^{(1)}$ is omitted for brevity. The $E_z^{(1)}$ and $H_\phi^{(1)}$ are the axial electric field and azimuthal magnetic field, respectively for region I, ω and k are the angular frequency and propagation constant for TM_{np} mode, respectively. $J_n(x)$ is the Bessel function of first kind of order n and $N_n(x)$ is the Bessel func-

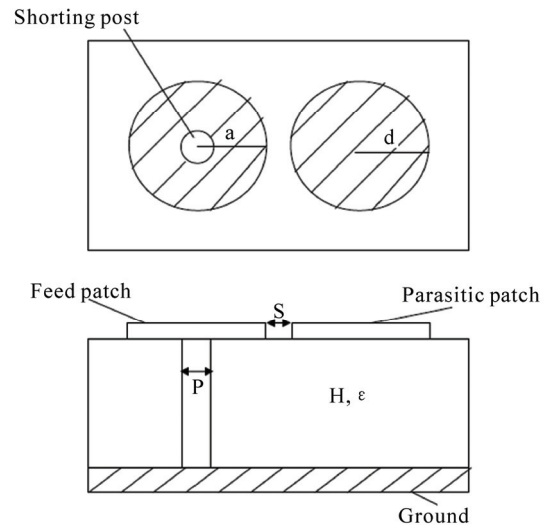


Figure 1. Geometrical configuration of the two gap-coupled circular microstrip patch antenna loaded with shorting post

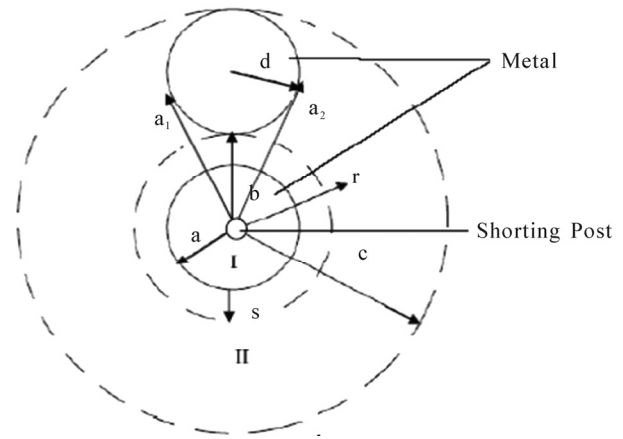


Figure 2. Analytical configuration of the two gap-coupled circular microstrip patch antenna loaded with shorting post

tion of second kind of order n . C_1 and C_2 are the amplitude constants for region I.

In region II ($b \leq r \leq c$):

The solution of the wave equation in cylindrical coordinates for region II gives the field expressions as:

$$E_z^{(2)} = -j\omega\mu[C_3J_n(kr) + C_4N_n(kr)]\cos n\varphi \quad (3)$$

$$H_\varphi^{(2)} = -k[C_3J'_n(kr) + C_4N'_n(kr)]\cos n\varphi \quad (4)$$

where C_3 and C_4 are the amplitude constants for region II. Considering the parasitic patch in isolation the boundary condition of vanishing $H_\varphi^{(2)}$ can be applied as:

$$H_\varphi^{(2)} = 0 \text{ for } b \leq r \leq c \text{ and } \alpha_1 \leq \varphi \leq \alpha_2 \quad (5)$$

Thus,

$$\frac{C_4}{C_3} = -\frac{\int_b^c J_n'(kr)rdr}{\int_b^c N_n'(kr)rdr} = \frac{I_2}{I_1} \quad (6)$$

Therefore the field expression in region II can be rewritten as:

$$E_z^{(2)} = -j\omega\mu C_n^{(2)} F_n^{(2)}(kr)\cos n\varphi \quad (7)$$

$$H_\varphi^{(2)} = -kC_n^{(2)} F_n^{(2)'}(kr)\cos n\varphi \quad (8)$$

where $C_n^{(2)}$ is a constant dependant on given mode n and

$$F_n^{(2)}(kr) = J_n(kr)I_1 - I_2N_n(kr) \quad (9)$$

Similarly,

$$E_z^{(1)} = 0 \quad \text{for } r = p/2$$

$$\frac{C_1}{C_2} = -\frac{N_n(kp/2)}{J_n(kp/2)} = \frac{I_3}{I_4}$$

Thus the field expression in region I is:

$$E_z^{(1)} = -j\omega\mu C_n^{(1)} F_n^{(1)}(kr)\cos n\varphi \quad (10)$$

$$H_\varphi^{(1)} = -kC_n^{(1)} F_n^{(1)'}(kr)\cos n\varphi \quad (11)$$

where $C_n^{(1)}$ is a constant and

$$F_n^{(1)}(kr) = J_n(kr)I_3 - N_n(kr)I_4 \quad (12)$$

We now consider the gap between two regions at the point of coupling between two patches as a π -type network [15] as shown in Figure 3.

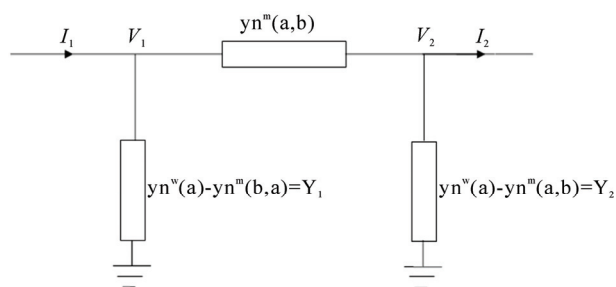


Figure 3. An equivalent circuit diagram of the two gap-gap coupled circular microstrip patch antenna

In Figure 3, $y_n^w(a/b)$ are the wall admittances of individual patches and $y_n^m(a,b)$ is the mutual admittance between the two patches.

Here,

$$y_n^m = \frac{1}{j\omega M}$$

where M denotes magnetic coupling and is given by

$$M = \int_0^h \int_0^q \frac{\mu_0}{4\pi \times s} dl_1 dl_2$$

where h is the substrate height and q is a correction factor. The formula for magnetic coupling is derived for infinitely thin cylindrical lines. However, to take account for substantial area of each cylinder an empirical correction factor is utilized. From the condition of discontinuity of current in these two regions, we can write:

$$aH_\varphi^{(1)}(a) - bH_\varphi^{(2)}(b) = -E_z^{(1)}(a)Y_1 - E_z^{(2)}(b)Y_2 \quad (13)$$

using this expression, we obtain:

$$\frac{C_n^{(2)}}{C_n^{(1)}} = \frac{aF_n^{(1)'}(ka) + \frac{j\omega\mu}{k}F_n^{(1)}(ka)Y_1}{bF_n^{(2)'}(kb) - \frac{j\omega\mu}{k}F_n^{(2)}(kb)Y_2} \quad (14)$$

For small gap normal component of electric field is continuous at r' where $r' = \frac{b+a}{2}$.

Therefore $E_z^{(1)}(r) = E_z^{(2)}(r)$ at $r = r'$.

From this

$$\frac{C_n^{(2)}}{C_n^{(1)}} = \frac{F_n^{(1)}(kr')}{F_n^{(2)}(kr')} \quad (15)$$

Equating Expressions (14) and (15) we get:

$$\frac{F_n^{(1)}(kr')}{F_n^{(2)}(kr')} - \frac{aF_n^{(1)}(ka) + \frac{j\omega\mu}{k} F_n^{(1)}(ka)Y_1}{bF_n^{(2)}(kb) - \frac{j\omega\mu}{k} F_n^{(2)}(kb)Y_2} = 0 \quad (16)$$

The above transcendental equation gives the resonant frequency of a given TM_{np} mode.

4. Results and Discussion

The proposed simulation model of two gap-coupled circular microstrip patch antenna is as shown in Figure 1. It is clearly seen that, for the short-circuited patch antenna, the input impedance become very sensitive to the feed position and strongly depends on the distance between the shorting post and the feed position [2–10]. The determination of all relevant parameters for the shorting post microstrip patch antenna is straight forward once the resonant frequency has been determined. It has been shown that the resonant frequency depends critically on dimension of the shorting post and gap distance between adjacent edges of the feed patch and parasitic patch.

In Figure 4, the variation of resonant frequency of different modes with radius of shorting post in feed patch is shown. It is important to note that at a fixed frequency, the patch size can be increased or decreased, depending on the radius of the shorting post. As the radius of the shorting post increases the resonance frequency of the proposed antenna is increases for TM_{01} TM_{11} and TM_{21} modes as shown in Figure 4 In Figure 5, the variation of resonant frequency of different modes with gap distance between adjacent edges of the feed patch and parasitic patch is shown. The resonant frequency decreases with increasing the gap distance between adjacent edges of the feed patch and parasitic patch for TM_{01} TM_{11} and TM_{21} modes as shown in Figure 5. The proposed antenna is also simulated using IE3D simulator. The numerically computed and simulated results are compared which shows good agreement as shown in Figure 4 and Figure 5.

The diameter of the shorting post and the gap distance between the adjacent edges of feed patch and parasitic patch also play an important role in the overall size of the patch conductor. Basically, the shorting post is modeled as an inductance parallel to the resonant LC circuit describing a reference resonant mode of the unloaded (without shorting post) patch. In an equivalent circuit, new resonance mode (with shorting post) can be viewed as resulting from the inductance due to shorting post. Using the resonant frequency of TM_{01} mode, the size of the gap-coupled circular microstrip antenna can be reduced for same frequency applications, because the resonant frequency of this mode is much less than the resonant frequencies of the conventional gap-coupled circular microstrip antenna presented in [15]. By varying the various parameters such as diameter of shorting post and the gap distance between adjacent edges, the reso-

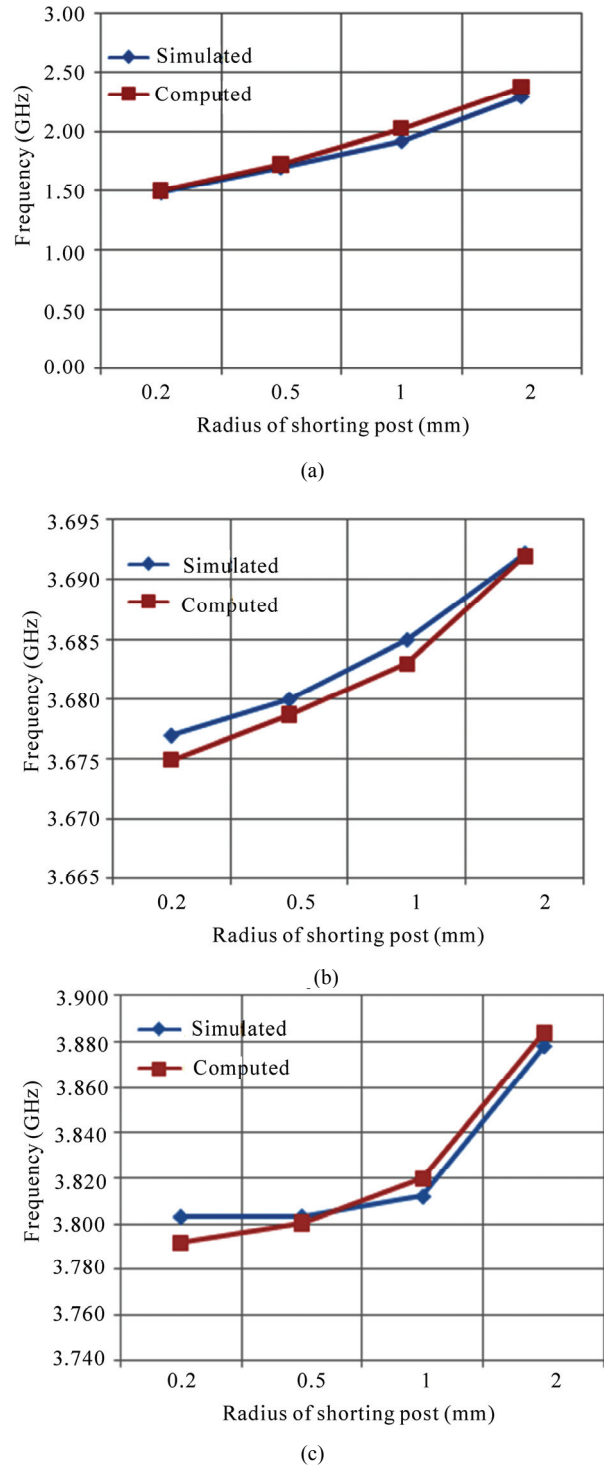
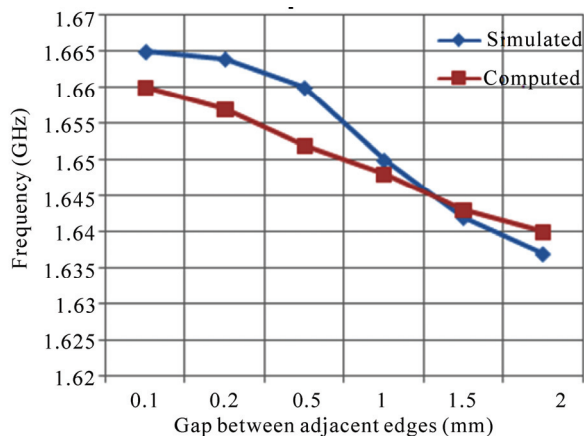


Figure 4. Variation of the resonant frequency with radius of the shorting post of the proposed antenna for, (a) TM_{01} mode with $s = 0.5$ mm; (b) TM_{11} mode with $s = 0.5$ mm and (c) TM_{21} mode with $s = 0.5$ mm

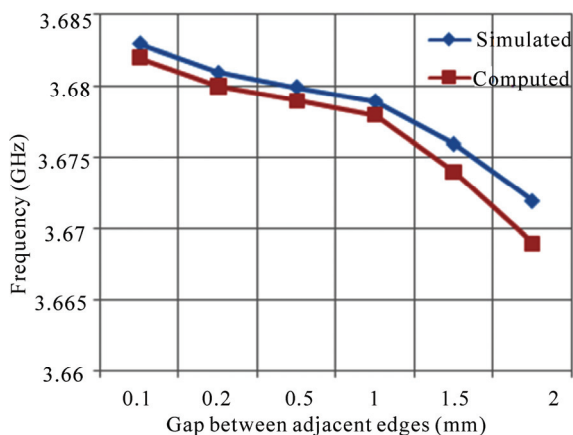
nant frequencies of the presented antenna can be controlled.

To validate the presentation of mode numbers the

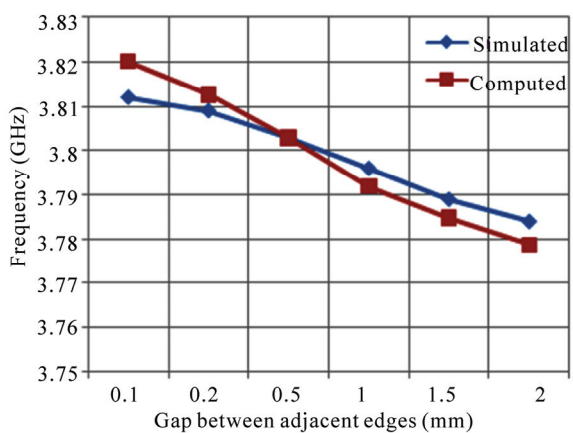
simulated current density on the patches are presented in Figure 6, 7 and 8. It is seen that the mode numbers are



(a)



(b)



(c)

Figure 5. Variation of the resonant frequency with gap distance between adjacent edges of the feed patch and parasitic patch for (a) TM_{01} mode with radius of shorting post = 0.5 mm, (b) TM_{11} mode with radius of shorting post = 0.5 mm, and (c) TM_{21} mode with radius of shorting post = 0.5 mm

predicted accurately. In this case, the current density towards ‘Red’ colour is maximum and current density towards ‘Blue’ colour is minimum. The current density represented by ‘Yellow’ colour is between the ‘Red’ and ‘Blue’. The left hand side patch is the feed patch and the right side patch is parasitic patch. In Figure 6, the yellow region is at the center of the feed patch and blue region at the surroundings of the green region conveys the TM_{01} mode. In Figure 7, it is seen that on the feed patch a yellow region and a blue region exists. This accounts for TM_{11} mode. Two blue regions in Figure 8 convey the existence of TM_{21} mode.

5. Conclusions

In this paper, a numerical model for shorting post loaded two gap-coupled circular microstrip patch antenna is developed. The comparison between the numerically computed and simulated results shows good agreement in resonant frequency for TM_{01} , TM_{11} , and TM_{21} modes. The proposed gap-coupled microstrip antennas loaded

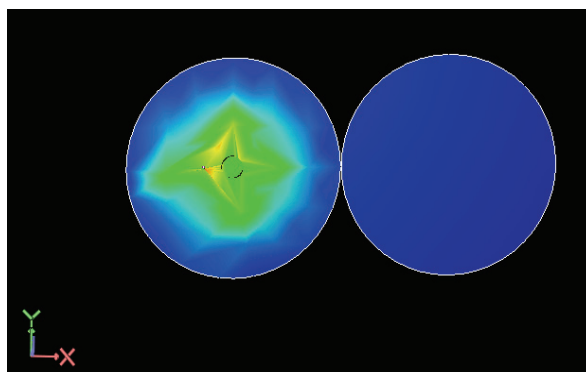


Figure 6. The current density distribution on the proposed two gap-coupled circular microstrip patch antennas loaded with shorting post for TM_{01} mode at frequency 2.149 GHz for gap distance between adjacent edges of feed patch and parasitic patch 0.1 mm and radius of shorting post 1.5 mm

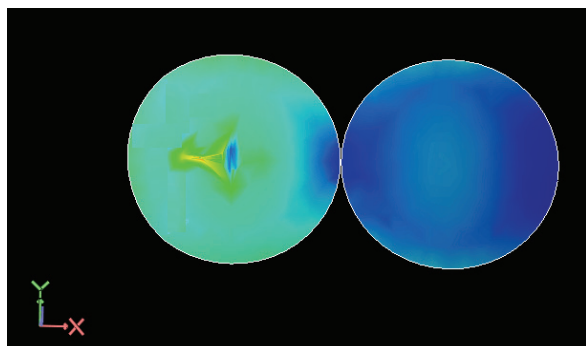


Figure 7. The current density distribution on the proposed two gap-coupled circular microstrip patch antennas loaded with shorting post for TM_{11} mode at frequency 3.6912 GHz for gap distance between adjacent edges of feed patch and parasitic patch 0.1 mm and radius of shorting post 1.5 mm

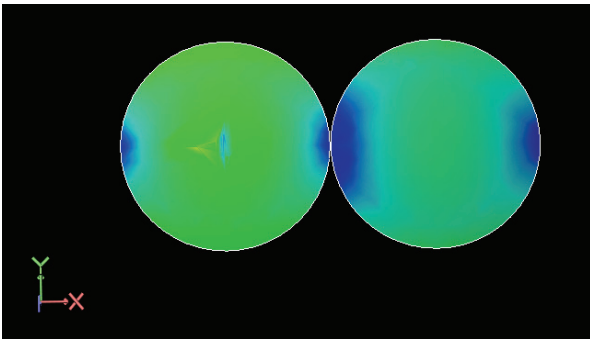


Figure 8. The current density distribution on the proposed two gap-coupled circular microstrip patch antennas loaded with shoring post for TM_{21} mode at frequency 3.8474 GHz for gap distance between adjacent edges of feed patch and parasitic patch 0.1 mm and radius of shoring post 1.5 mm

with shoring post can be used for multi frequency applications. Also the size of the proposed antenna can be controlled by varying either gap distance between adjacent edges of the feed patch and parasitic patch or radius of the shoring post. The proposed model can be extended to multiple resonators as well as analysis with different patch sizes.

6. Acknowledgement

Authors are sincerely thankful to the reviewers for critical comments and suggestions to improve the quality of the manuscript.

REFERENCES

- [1] M. Hirvonen, P. Pursula, K. Jaakkola, and K. Laukkanen, "Planer inverted F antenna for radio frequency identification," *Electronics Letter*, Vol. 40, No. 14, pp. 848–850, July 2004.
- [2] A Sharma and G. Singh, "Design of single pin shorted three-dielectric-layered substrates rectangular patch microstrip antenna for communication systems," *Progress In Electromagnetic Research Letters*, Vol. 2, pp. 157–165, 2008.
- [3] R. Garg, P. Bhartia, I. Bahl, and A. Ittipiboon, "Microstrip Antenna Design Handbook," Artech House: London, 2001.
- [4] T. Chakravarty, S. Biswas, A. Majumdar, and A. De, "Computation of resonant frequency of annularing-loaded circular patch", *Microwave and Optical Technology Letter*, Vol. 48, No. 3, pp. 622–626, 2006.
- [5] D. M. Pozar, "Microstrip antennas," *Proceedings of the IEEE*, Vol. 80, No. 1, pp. 79–91, January 1992.
- [6] P Kumar, G. Singh, and S. Bhooshan, "Gap-coupled microstrip antennas," *Proceedings of the International Conference on Computational Intelligence and Multimedia Application, India*, pp. 434–437, 2007.
- [7] K. P Ray, S. Ghosh, and K. Nirmala, "Compact broadband gap-coupled microstrip antennas," *Proceedings of International Symposium on IEEE Antennas and Propagation Society*, pp. 3719–3722, July 2006.
- [8] R. B. Waterhouse, S. D. Targonski, and D. M. Kokoto, "Design and performance of small printed antennas," *IEEE Transactions on Antennas Propagation*, Vol. 46, pp. 1629–1633, 1998.
- [9] T. K. Lo, C.-O. Ho, Y. Hwang, E. K. W. Lam, and B. Lee, "Miniature aperture-coupled microstrip antenna of very high permittivity," *Electronics Letter*, Vol. 33, pp. 9–10, January 1997.
- [10] R. Porath, "Theory of miniaturized shoring post microstrip antennas," *IEEE Trans. Antennas Propagation*, Vol. 48, No. 1, pp. 41–47, January 2000.
- [11] C.-L. Tang, H.-T. Chen, and K.-L. Wong, "Small circular microstrip antenna with dual frequency operation," *Electronics Letter*, Vol. 33, No. 73, pp. 1112–1113, 1997.
- [12] K.-L. Wong and W.-S. Chen, "Compact microstrip antenna with dual-frequency operation," *Electronics Letter*, Vol. 33, No. 8, pp. 646–647, April 1997.
- [13] T. Chakravarty and A. De, "Investigation of modes tunable circular patch radiator with arbitrarily located shoring posts," *IETE Technical Review*, Vol. 16, No. 1, pp. 109–111, January 1999.
- [14] T. Chakravarty and A. De, "Design of tunable modes and dual-band circular patch antenna using shoring posts," *IEEE Proceeding Microwaves, Antennas Propagation*, Vol. 146, No. 3, pp. 224–228, 1999.
- [15] P. Kumar, T. Chakravarty, G. Singh, S. Bhooshan, and S. K. Khah "Numerical computation of resonant frequency of gap coupled circular microstrip antennas," *Journal of Electromagnetic Waves and Applications*, Vol. 21, No. 10, pp. 1303–1311, 2007.
- [16] T. Chakravarty, S. M. Roy, S. K. Sanyal, and A. De, "A novel microstrip patch antenna with large impedance bandwidth. In VHF/UHF range," *Progress in Electromagnetics Research*, Vol. 54, pp. 83–93, 2005.